Nonlinear structure-enhancing filtering using plane-wave prediction[a]

[a]Published in Geophysical Prospecting, 58, 415-427, (2010)

Yang Liu[*†], *Sergey Fomel*[†], *Guochang Liu*[‡]

ABSTRACT

Attenuation of random noise and enhancement of structural continuity can significantly improve the quality of seismic interpretation. We present a new technique, which aims at reducing random noise while protecting structural information. The technique is based on combining structure prediction with either similarity-mean filtering or lower-upper-middle (LUM) filtering. We use structure prediction to form a structural prediction of seismic traces from neighboring traces. We apply a nonlinear similarity-mean filter or an LUM filter to select best samples from different predictions. In comparison with other common filters, such as mean or median, the additional parameters of the nonlinear filters allow us to better control the balance between eliminating random noise and protecting structural information. Numerical tests using synthetic and field data show the effectiveness of the proposed structure-enhancing filters.

INTRODUCTION

Extracting structural information is the most important goal of seismic interpretation. A number of approaches have been proposed to preserve and enhance structural information. Hoeber et al. (2006) applied nonlinear filters, such as median, trimmed mean, and adaptive Gaussian, over planar surfaces parallel to the structural dip. Fehmers and Höcker (2003) and Hale (2009) applied structure-oriented filtering based on anisotropic diffusion. Fomel and Guitton (2006) suggested the method of plane-wave construction. AlBinHassan et al. (2006) developed 3-D edge-preserving smoothing (EPS) operators to reduce noise without blurring sharp discontinuities. Traonmilin and Herrmann (2008) used a mix of finite-impulse-response (FIR) and infinite-impulse-response (IIR) filters, followed by f-x filtering, to perform structure-preserving seismic processing. Whitcombe et al. (2008) introduced a frequency-dependent, structurally conformable filter. Random noise attenuation and structure protection are always ambivalent problems in seismic data processing. The main challenge in designing effective structure-enhancing filters is controlling the balance between noise attenuation and signal preservation.

Mean filter (stacking) plays an important role in improving signal-to-noise ratio in seismic data processing (Yilmaz, 2001). Conventional stacking is a simple

and effective method of denoising, but it is optimal only when noise has a Gaussian distribution (Mayne, 1962). Therefore, alternative stacking methods were proposed. Robinson (1970) proposed a signal-to-noise-ratio-based weighted stack to further minimize noise. Tyapkin and Ursin (2005) developed optimum-weighted stacking. To eliminate artifacts in angle-domain common-image gathers, Tang (2007) presented a selective-stacking approach, which applied local smoothing of envelope function to achieve the weighting function. Rashed (2008) proposed "smart stacking," which is based on optimizing seismic amplitudes of the stacked signal by excluding harmful samples from the stack and applying more weight to the center of the samples population. Liu et al. (2009a) introduced time-dependent smooth weights to design a similarity-mean stack, which is a nonstationary, nonlinear operator.

Lower-upper-middle (LUM) filters (Hardie and Boncelet, 1993) are a class of rank-order-based filters that generalize the concept of the median filter. They combine the characteristics of two subclasses, LUM smoothers and LUM sharpeners, and find a variety of signal and image-processing applications. A special LUM smoother, probably still the most widely used, is a simple median of the points within a window. The median filter is a well-known method that can effectively suppress spike-like noise in nonstationary signal processing. Median filters find important applications in seismic data analysis. Mi and Margrave (2000) incorporated noise reduction using median filter into standard Kirchhoff time migration. Zhang and Ulrych (2003) used a hyperbolic median filter to suppress multiples. Liu et al. (2006, 2009b) implemented random-noise attenuation using 2-D multistage median filter and nonstationary time-varying median filter. However, in many cases the median filter introduces too much smoothing. LUM sharpeners have excellent detail preserving characteristics because of their ability to pass small details with minimal distortion. For a given window size and shape, the parameters of LUM filter can be adjusted independently to yield a wide range of characteristics.

In this paper, we combine structure prediction (Fomel, 2008) with either nonlinear similarity-mean filtering or lower-upper-middle (LUM) filtering to define a structure-enhancing filter. Structure prediction generates structure-conforming predictions of seismic events from neighboring traces, whereas a similarity-mean filtering or an LUM filtering reduces several predictions to optimal output values. We test the proposed method on synthetic and field data examples to demonstrate its ability to enhance structural details of seismic images.

THEORY

Structure prediction

The method of plane-wave destruction (Claerbout, 1992) uses a local plane-wave model for characterizing the structure of seismic data. It finds numerous applications in seismic imaging and data processing (Fomel, 2002). Letting a seismic section, $\mathbf{s}$,

be a collection of traces, $\mathbf{s} = [\mathbf{s}_1\ \mathbf{s}_2\ \dots\ \mathbf{s}_N]^T$, the plane-wave destruction operation can be defined in a linear operator notation as

$$\mathbf{d} = \mathbf{D}(\sigma)\,\mathbf{s}\ , \tag{1}$$

where $\mathbf{d}$ is the destruction residual and $\mathbf{D}$ is the nonstationary plane-wave destruction operator defined as follows

$$\begin{bmatrix} \mathbf{d}_1 \\ \mathbf{d}_2 \\ \mathbf{d}_3 \\ \cdots \\ \mathbf{d}_N \end{bmatrix} = \begin{bmatrix} \mathbf{I} & 0 & 0 & \cdots & 0 \\ -\mathbf{P}_{1,2}(\sigma_1) & \mathbf{I} & 0 & \cdots & 0 \\ 0 & -\mathbf{P}_{2,3}(\sigma_2) & \mathbf{I} & \cdots & 0 \\ \cdots & \cdots & \cdots & \cdots & \cdots \\ 0 & 0 & \cdots & -\mathbf{P}_{N-1,N}(\sigma_{N-1}) & \mathbf{I} \end{bmatrix} \begin{bmatrix} \mathbf{s}_1 \\ \mathbf{s}_2 \\ \mathbf{s}_3 \\ \cdots \\ \mathbf{s}_N \end{bmatrix}\ , \tag{2}$$

where $\mathbf{I}$ stands for the identity operator, σ_i is local dip pattern, and $\mathbf{P}_{i,j}(\sigma_i)$ is an operator for prediction of trace j from trace i according to the dip pattern σ_i. A trace is predicted by shifting it according to the local seismic event slopes. Minimizing the destruction residual $\mathbf{d}$ provides a method of estimating the local slopes σ (Fomel, 2002).

The least-squares minimization of $\mathbf{d}$ is achieved by using iterative conjugate-gradient (CG) method and smooth regularization. Local dip at a fault position cannot be accurately estimated, its value will depend on the initial slope estimate and regularization.

Prediction of a trace from a distant neighbor can be accomplished by simple recursion, i.e., predicting trace k from trace 1 is simply

$$\mathbf{P}_{1,k} = \mathbf{P}_{k-1,k}\ \cdots\ \mathbf{P}_{2,3}\,\mathbf{P}_{1,2}\ . \tag{3}$$

Fomel (2008) applied plane-wave prediction to predictive painting of seismic images. In this paper, we use a similar construction to recursively predict a trace from its neighbors.

An example is shown in Figure 1a. The input data is borrowed from Claerbout (2008): a synthetic seismic image containing dipping beds, an uncomformity, and a fault. Figure 1b shows the same image with Gaussian noise added. Figure 1c shows local slopes measured from the noisy image by plane-wave destruction. The estimated slope field correctly depicts the constant slope in the top part of the image and the sinusoidal variation of slopes in the bottom. In the next step, we predict every trace from its neighbor traces according to the local slope, as described by Fomel (2008). We chose a total of 14 prediction steps (7 from the left and 7 from the right), which, with the addition of the original section, generated a data volume (Figure 1d). The prediction axis corresponds to index k in equation 3. The volume is flat along the prediction direction, which confirms the ability of plane-wave destruction to follow the local structure. However, it still contains some discontinuous information because of the faults. In the next step, we apply nonlinear structure-enhancing filtering to process the data along the prediction direction.

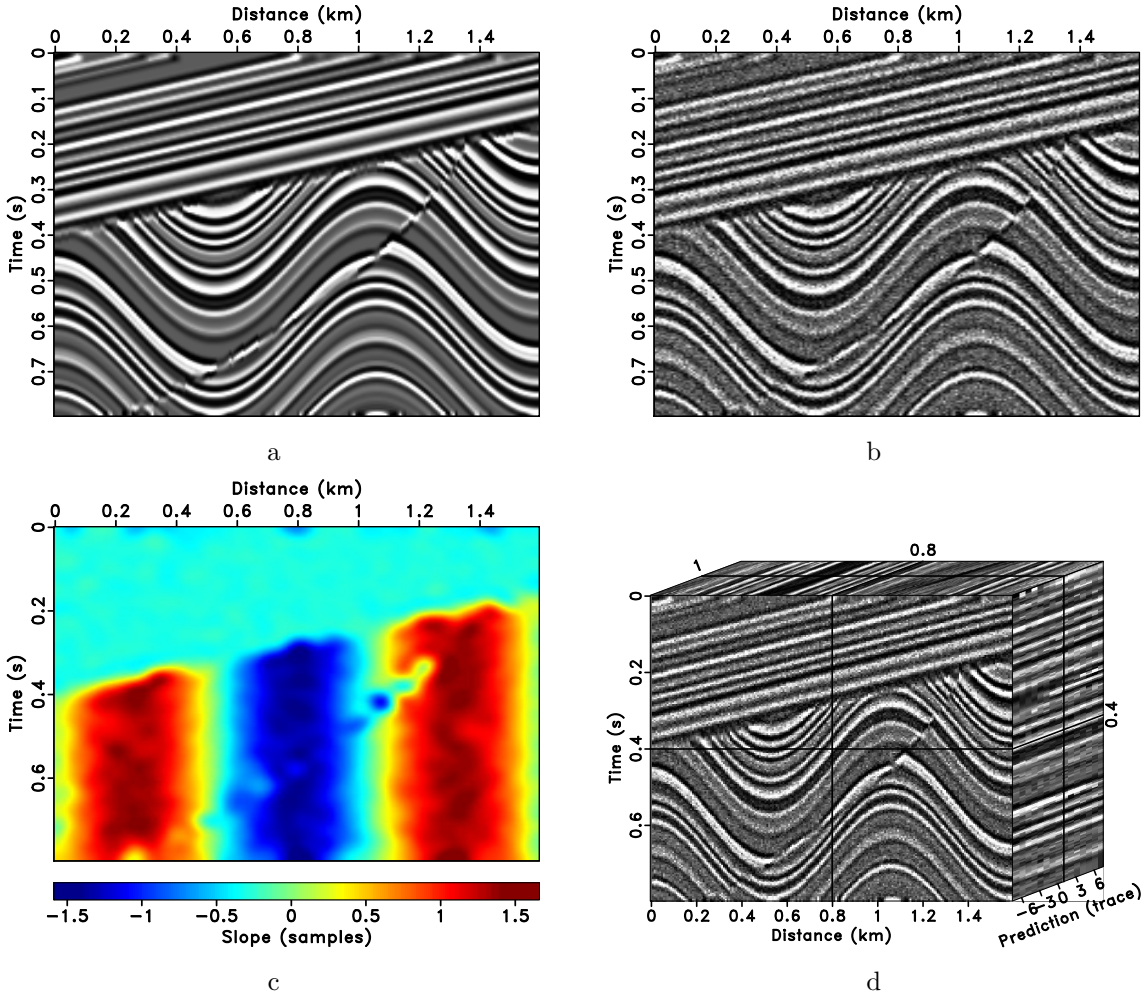

Figure 1: Noise-free synthetic image (a), noisy image (b), local slopes estimated from Figure 1b (c), and predictive data volume, where every trace is supplemented with predictions from its neighbors (d).

Choices of nonlinear filters

We have tried two different choices to select best samples from prediction data volume: Gaussian similarity-mean filter and lower-upper-middle (LUM) filter.

Gaussian similarity-mean filter

The similarity-mean filter is a nonlinear filter that uses local correlation coefficients as desired weight coefficients (Liu et al., 2009a). It is described in Appendix A. We chose the shaping operator with smoothing radius of 10 samples in time to calculate local similarity coefficients between the predicted data at each prediction step and original data (reference data). Figure 2a displays similarity-weight coefficients from local correlation. The elements with the shortest prediction distance get largest weights because they provide the most accurate prediction and therefore are most similar to the original image. We used zero-value boundary conditions for the prediction, so the predicted amplitudes from the left most and the right most sides are zero. This results in the similarity coefficients on the corners of the weight cube to be zero. In the weighted mean filter, large weight coefficients get selected when the similarity is strong between processed data and reference data. We introduce additionally Gaussian weights to localize the smoothing characteristics of the filter

$$w_i = e^{-h_i^2/h_r^2} \,, \tag{4}$$

where h_i is the distance to trace i and h_r is the reference parameter that controls the shape of the weight function. This construction is analogous to bilateral or non-local filtering (Tomasi and Manduchi, 1998; Gilboa and Osher, 2008). Figure 2b shows the product of Gaussian weights and similarity weights. The prediction data volumes only with similarity weights applied and with Gaussian similarity weights applied are shown in Figure 2c and 2d respectively. After applying Gaussian and similarity weights, we stack the data in Figure 2d along the prediction direction. The result is shown in Figure 3b.

For comparison, we used the standard mean filter to process the prediction data volume (Figure 1d) along the prediction direction. The result is shown in Figure 3a and corresponds, in this case, to simple box smoothing along the local image structure. The standard mean filter simply stacks all information along the prediction direction. It enhances structural continuity but smears information across the fault.

For further discussion, we show the difference between the noisy image (Figure 1b) and structure-enhancing results with the standard mean filter and the Gaussian similarity-mean filter (Figure 3a and 3b). We kept the same scale of magnitude and plotting clips as that of the input image. From Figure 4a and 4b, the coherent events are well protected by the two methods because structure prediction can exactly predict coherent information. However fault information is destroyed by the mean filter (Figure 4a), while the similarity-mean filter provides a result where fault information is protected well, whereas random noise is attenuated (Figure 4b).

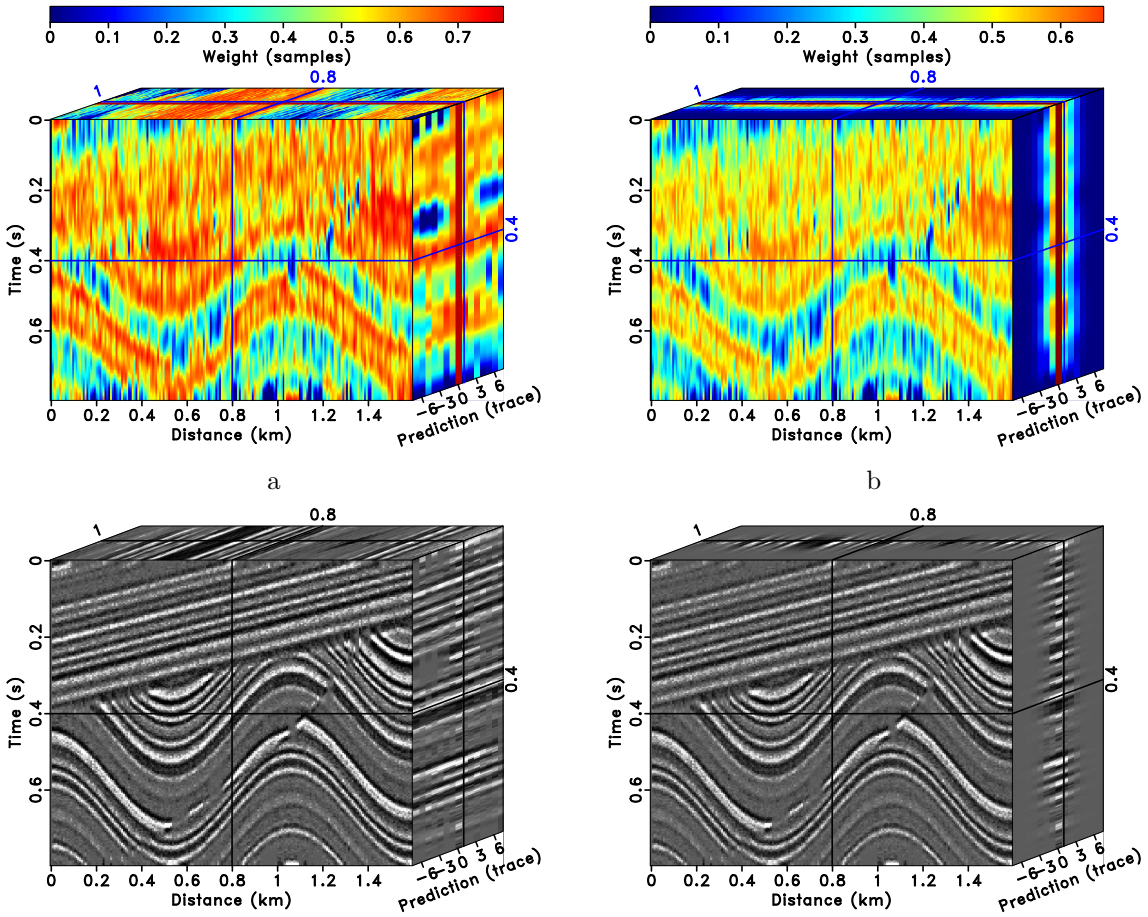

Figure 2: Similarity weights (a), product of Gaussian weights and similarity weights (b), the data only with similarity weights applied (c), and the data with Gaussian similarity weights applied (d).

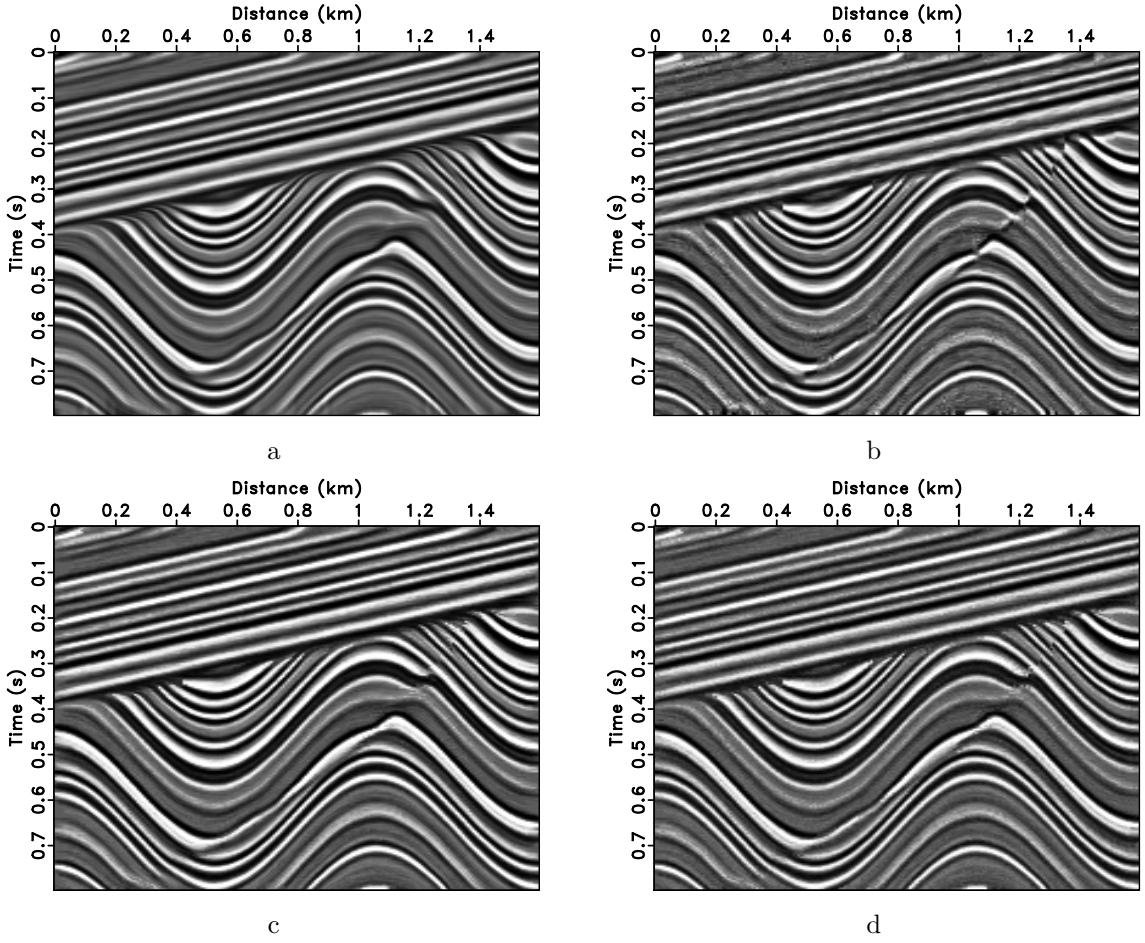

Figure 3: Structure-enhancing results using different methods. Standard mean filtering (a), similarity-mean filtering (b), standard median filtering with filter-window length 15 (c), and lower-upper-middle (LUM) filtering with parameters $k = l = 7$ (d).

Lower-upper-middle filter

The lower-upper-middle (LUM) filter is a nonlinear filter that is simple to define and yet effective for noise attenuation in non-stationary signal processing (Hardie and Boncelet, 1993). It has two parameters, one for smoothing and the other for sharpening. A general class of LUM filters includes LUM smoothers and LUM sharpeners as special cases (Appendix B).

By manipulating the parameters k (for smoothing) and l (for sharpening), the lower-upper-middle (LUM) filter takes on a variety of characteristics. We found that $k = l = (N-1)/2$ works well for our synthetic and field data examples. In the synthetic example, special smoothing and sharpening parameters, $k = l = 7$, were chosen to balance the ability between noise attenuation and fault protection. After applying the LUM filter on the synthetic noisy image, we obtain the image shown in Figure 3d. Comparing with Figure 3b, the LUM filter displays the similar-quality result as Gaussian similarity-mean filter. However, the LUM filter is somewhat easier to control than the similarity-mean filter.

The standard median filter with filter-window length 15 is compared to the lower-upper-middle (LUM) filter. After applying the median filter on the prediction direction of Figure 1d, the result is shown in Figure 3c. When comparing with the mean filter (Figure 3a), the median filter has a better fault-protection ability but weaker noise-attenuation result. However, it still makes edges of some faults ambiguous. The LUM filter uses smoothing and sharpening parameters to limit the smoothing characteristics of the standard median filter. Therefore, it strikes a reasonable balance between structure enhancement and fault protection. Figure 4c and 4d show the difference between the noisy image (Figure 1b) and structure-enhancing results with the standard median filter (Figure 3c) and the LUM filter (Figure 3d). While coherent events can be preserved by either of the two filters, the median filter has a better result of fault protection than the mean filter (Figure 4c) and the LUM filter can further reduce the fault damage of the standard median filter (Figure 4d).

The key steps of our method are illustrated schematically in Figure 5.

FIELD DATA EXAMPLES

For the first field-data test, we use a time-migrated seismic image from a historic Gulf of Mexico dataset (Claerbout, 2008). The input is shown in Figure 6a. After estimating the field of local slopes (Figure 6b), we apply structure prediction to calculate the structural data volume (Figure 7a), which effectively flattens the data. As in the synthetic example, the length of the prediction axis is 15. Next, we apply two different filtering approaches. The first choice is the similarity-mean filter. We display the product of Gaussian weights and similarity weights in Figure 7b. After applying the similarity-mean filter, we can get a structure-enhanced image (Figure 8a): the fault structures are protected well while noise is removed. Our second choice is an

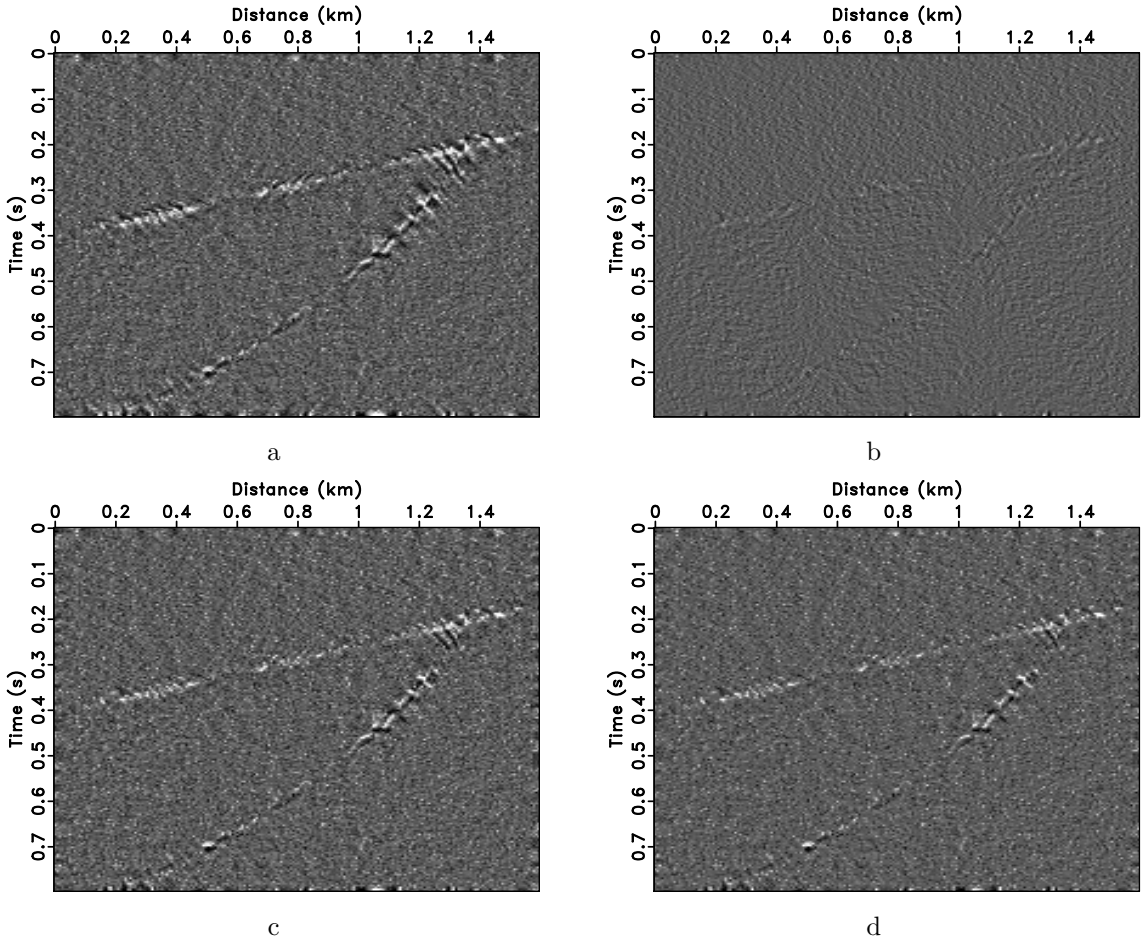

Figure 4: Difference between Figure 1b and structure-enhancing results (Figure 3). Standard mean filtering (a), similarity-mean filtering (b), standard median filtering (c), and lower-upper-middle (LUM) filtering (d).

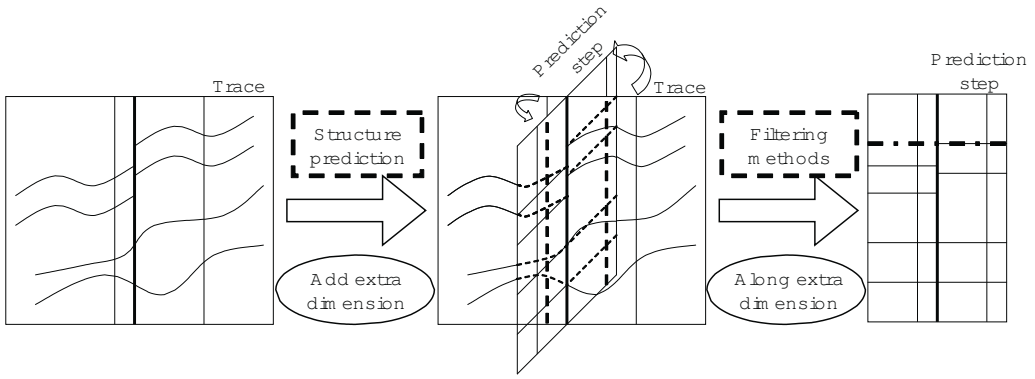

Figure 5: Schematic illustration of the proposed workflow.

lower-upper-middle (LUM) filter with parameters $k = l = 7$. The enhanced result is shown in Figure 8b. Similarly to the similarity-mean filter, the LUM filter highlights locally continuous reflectors while preserving the geometry of faults. Figure 9 shows the difference sections, in which the structure-enhancing results using two filtering methods (Figure 8) are subtracted from the original data (Figure 6a). After processing, the coherent events are preserved by both methods. The LUM filter also removes some short events with crossing dips.

An extension of the method to 3-D is straightforward and follows the 3-D predictive painting construction of Fomel (2008). We use a 3-D field data volume from the Gulf of Mexico to further test our methods (Figure 10). The dataset includes faults having an upside-down cone shape and some amount of random noise. Although variations in amplitude along reflectors can be stratigraphically significant, our goal is to enhance structurally continuous events. We chose a total of 24 prediction traces (2 prediction-step distances around the reference trace), which, with the addition of the original trace, generated a 4-D data volume. The corresponding inline and crossline dips were measured automatically from the image using plane-wave destruction (Figure 11 and 12). Dip sections display different tendencies in inline and crossline directions. Figure 13 and 14 show results of nonlinear structure-enhancing filtering. When processing along the prediction direction, both of our nonlinear filters work well for noise reduction and fault protection. Figure 15 and 16 show the difference sections between the original data (Figure 10) and the structure-enhancing results using two filtering methods (Figure 13 and 14). Similar to the results in the synthetic and 2-D field examples, both methods can protect useful information well.

CONCLUSION

We have introduced a new technique that combines structure prediction and signal-enhancing filters: similarity-mean filter and lower-upper-middle (LUM) filter, for attenuating random noise while enhancing structural information. The technique is generic. One can replace the proposed filters with other prediction and signal-enhancing filter methods. Experiments with synthetic and field data show that nonlinear structure-enhancing filters can both eliminate random noise and preserve fault information in seismic images. Our method makes an implicit assumption that data is made of long, coherent events and random noise. It may need a further improvement to deal with areas where either crossing dips or no coherent events are present.

ACKNOWLEDGMENTS

We thank Hongliu Zeng for useful discussions. We thank assistant editor Tijmen Jan Moser, associate editor Peter Hanssen, and two anonymous reviewers for their constructive comments and suggestions. We thank Texaco for providing the 3-D Gulf of Mexico dataset, and BGP Americas for partial financial support of this work. Pub-

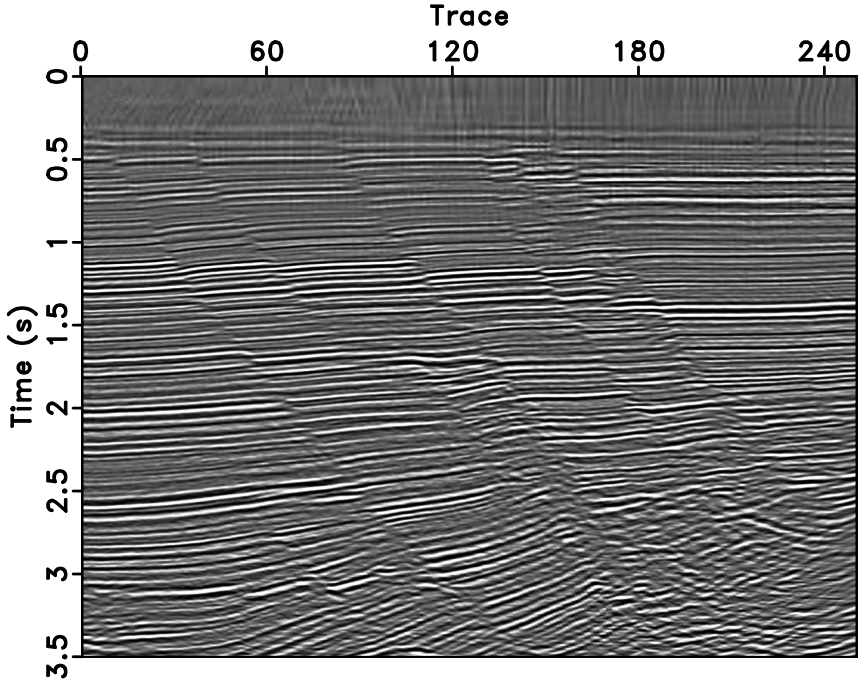

a

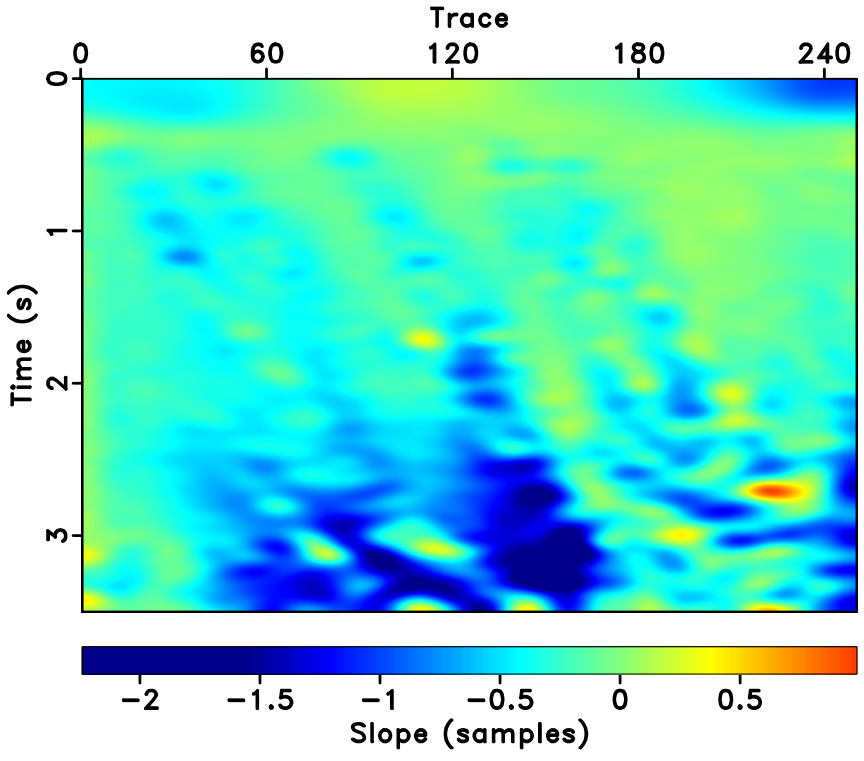

b

Figure 6: 2-D field data (a) and local slopes (b).

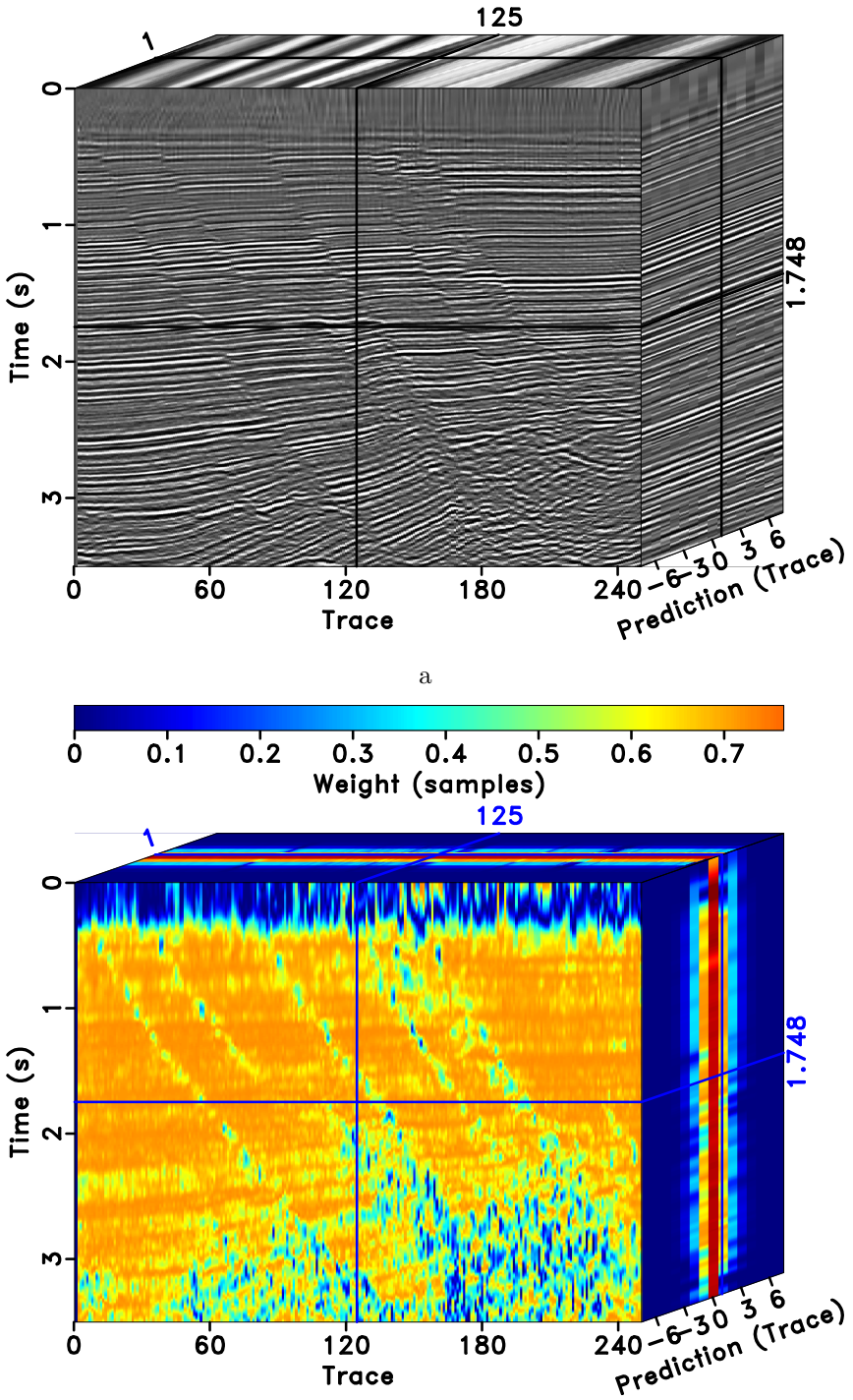

Figure 7: Predictive data volume (a) and product of Gaussian weights and similarity weights (b).

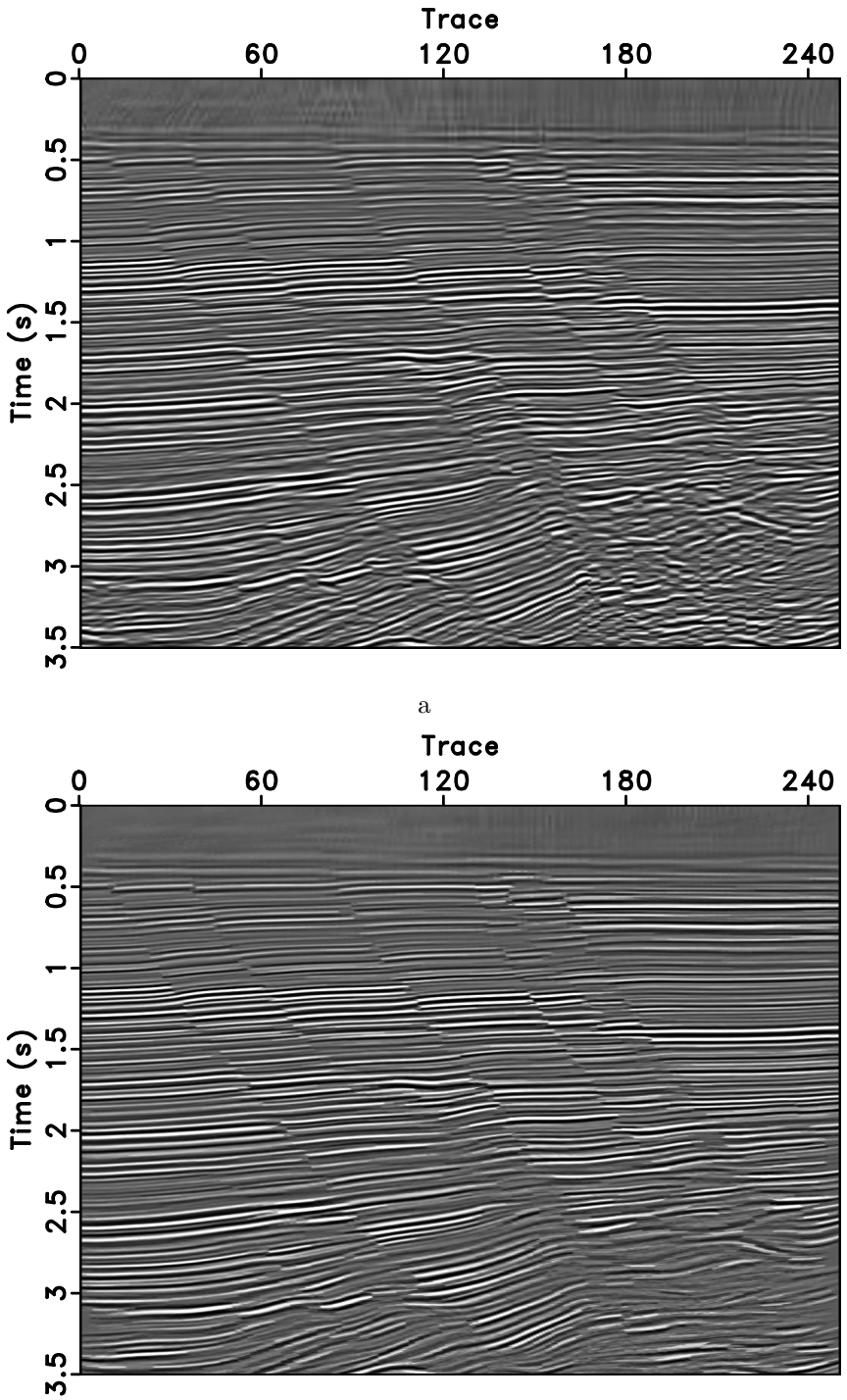

a

b

Figure 8: Structure-enhancing results for image from Figure 6a using similarity-mean filtering (a) and lower-upper-middle (LUM) filtering (b).

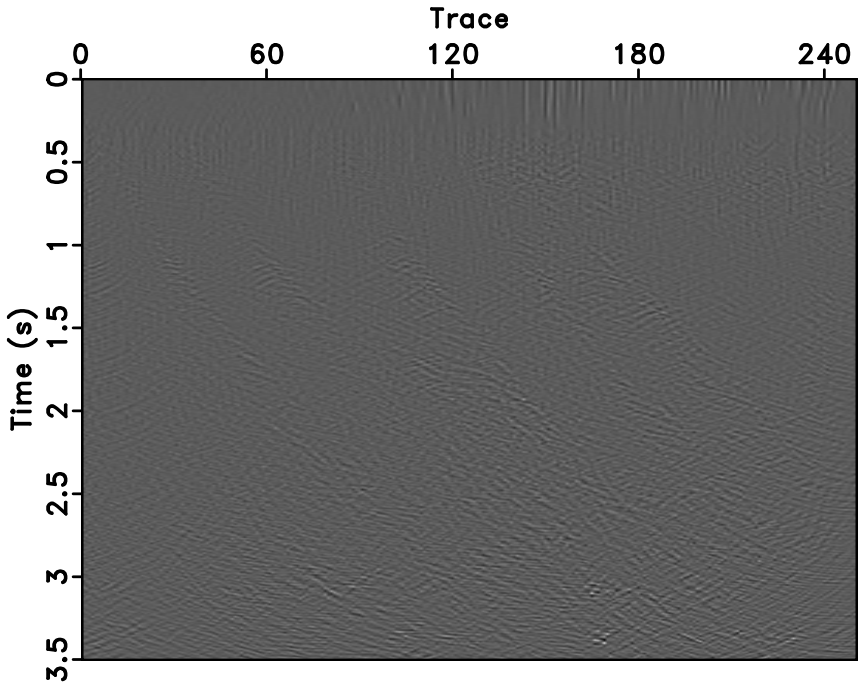

a

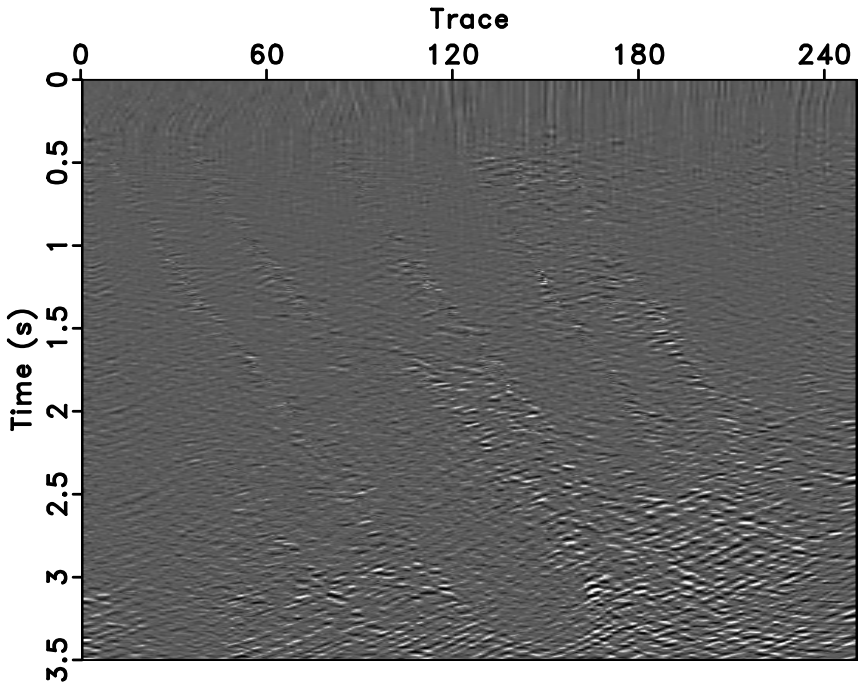

b

Figure 9: Difference between Figure 6a and structure-enhancing results (Figure 8). Similarity-mean filtering (a) and lower-upper-middle (LUM) filtering (b).

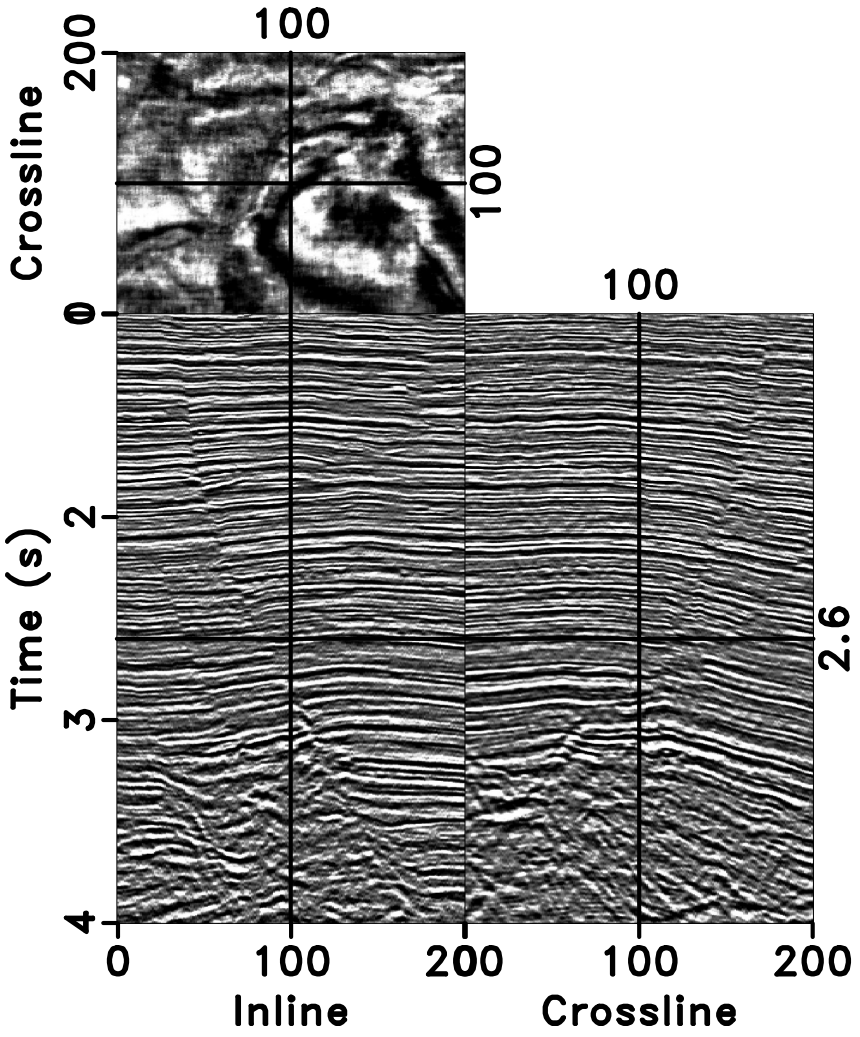

Figure 10: 3-D image from Gulf of Mexico.

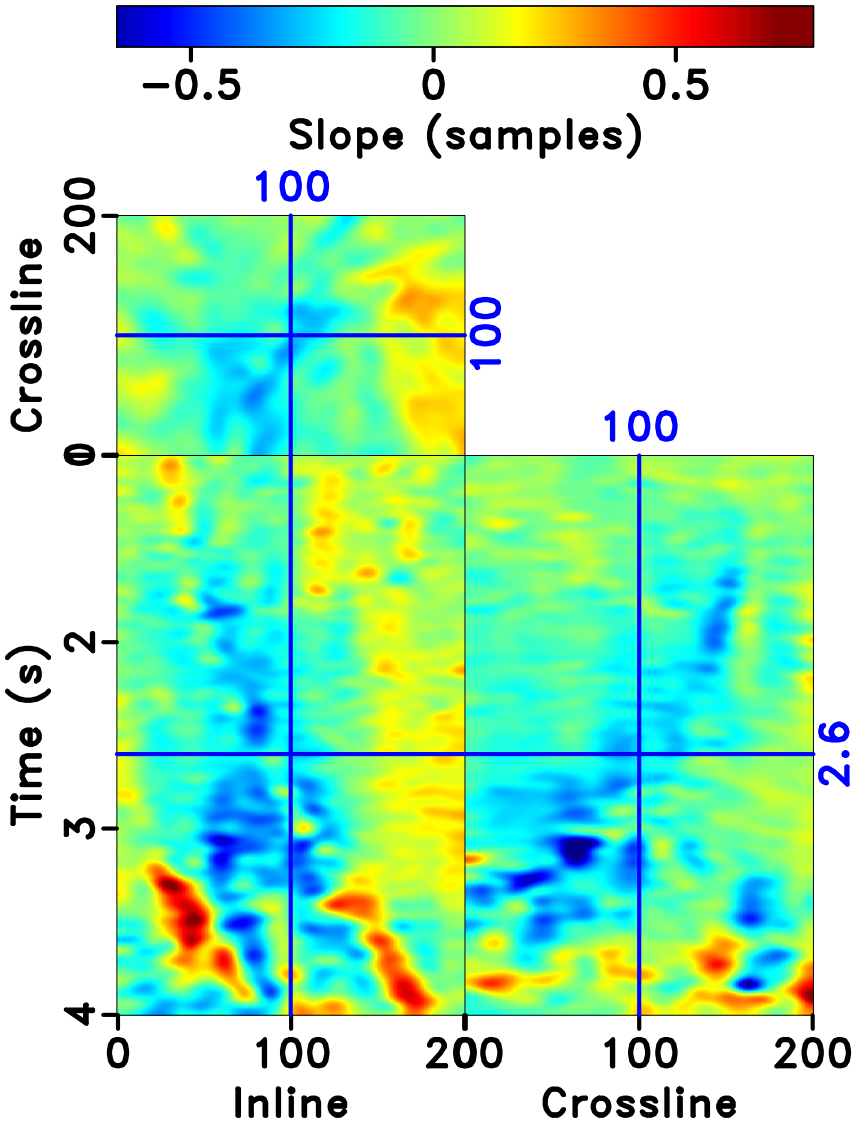

Figure 11: Local inline dip for the 3-D image from Figure 10.

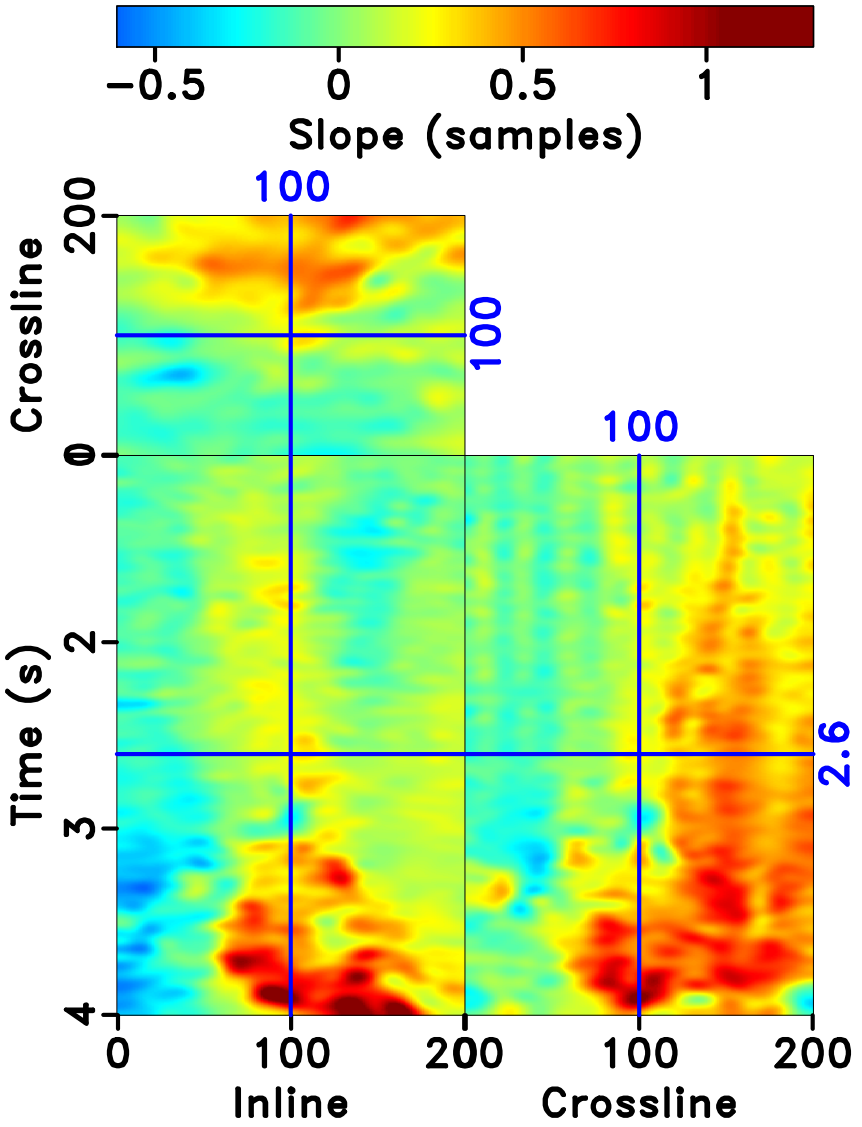

Figure 12: Local crossline dip for the 3-D image from Figure 10.

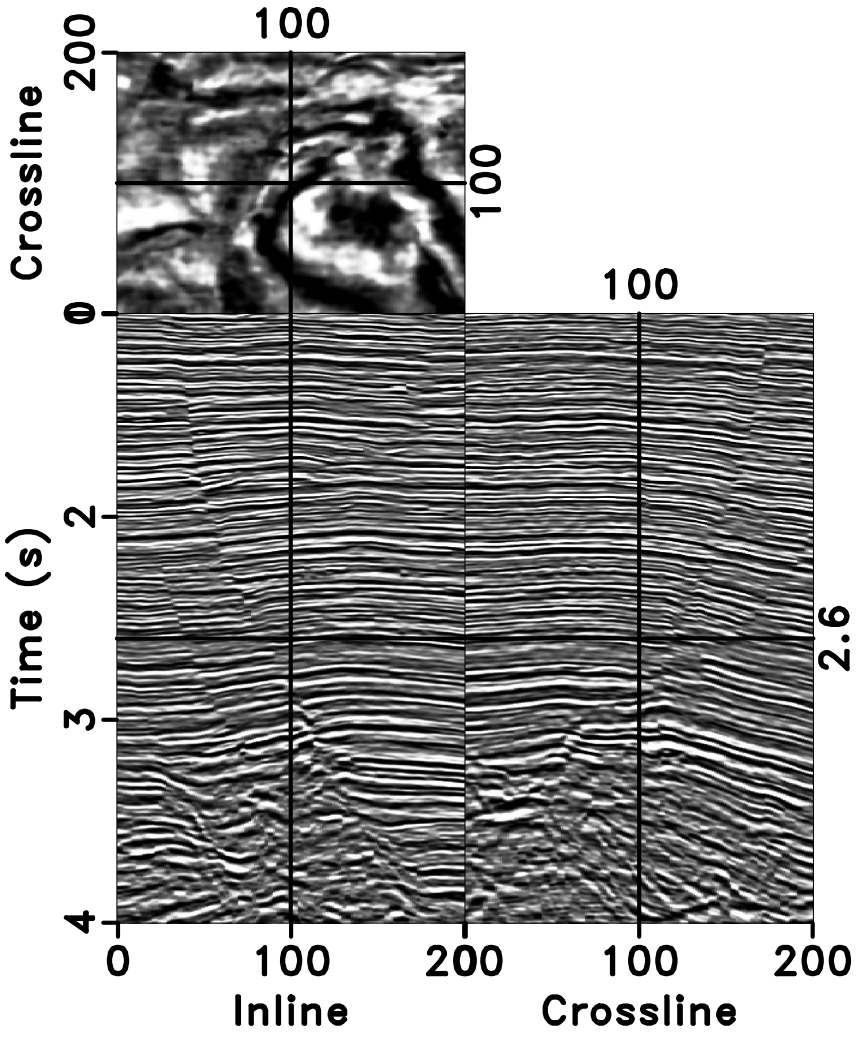

Figure 13: Structure-enhancing result using similarity-mean filtering. Compare with Figure 10.

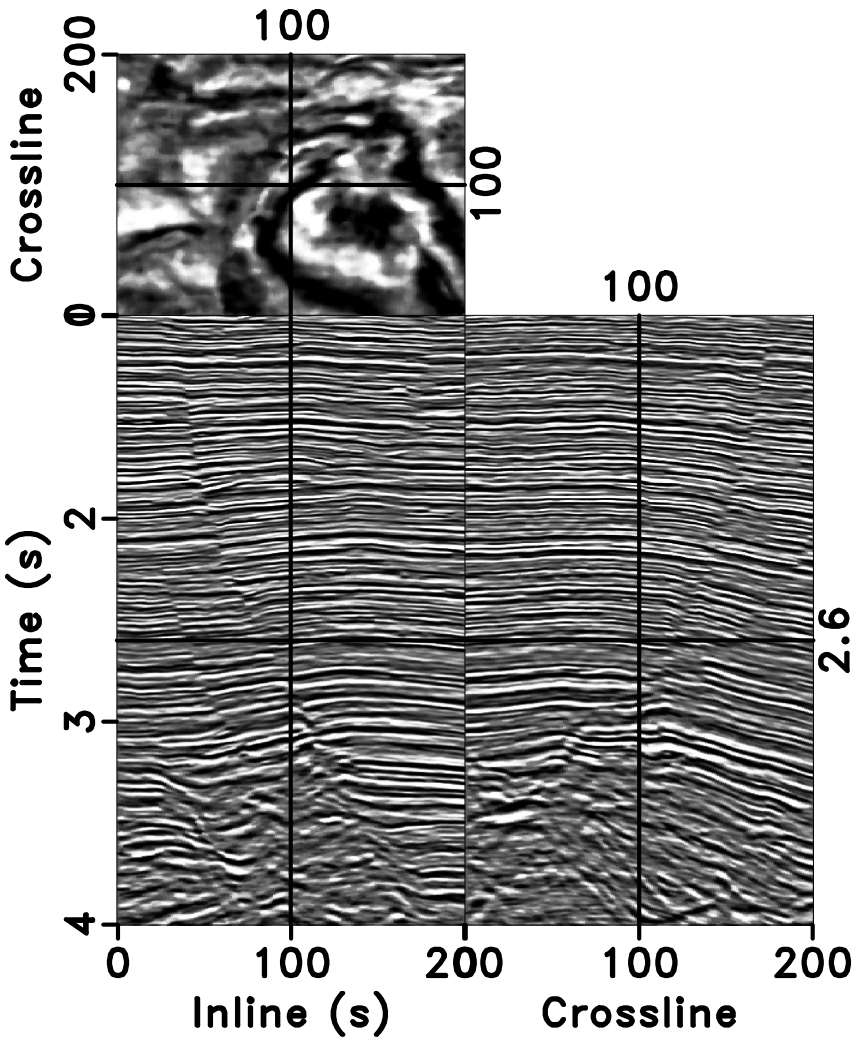

Figure 14: Structure-enhancing result using lower-upper-middle (LUM) filtering. Compare with Figure 10.

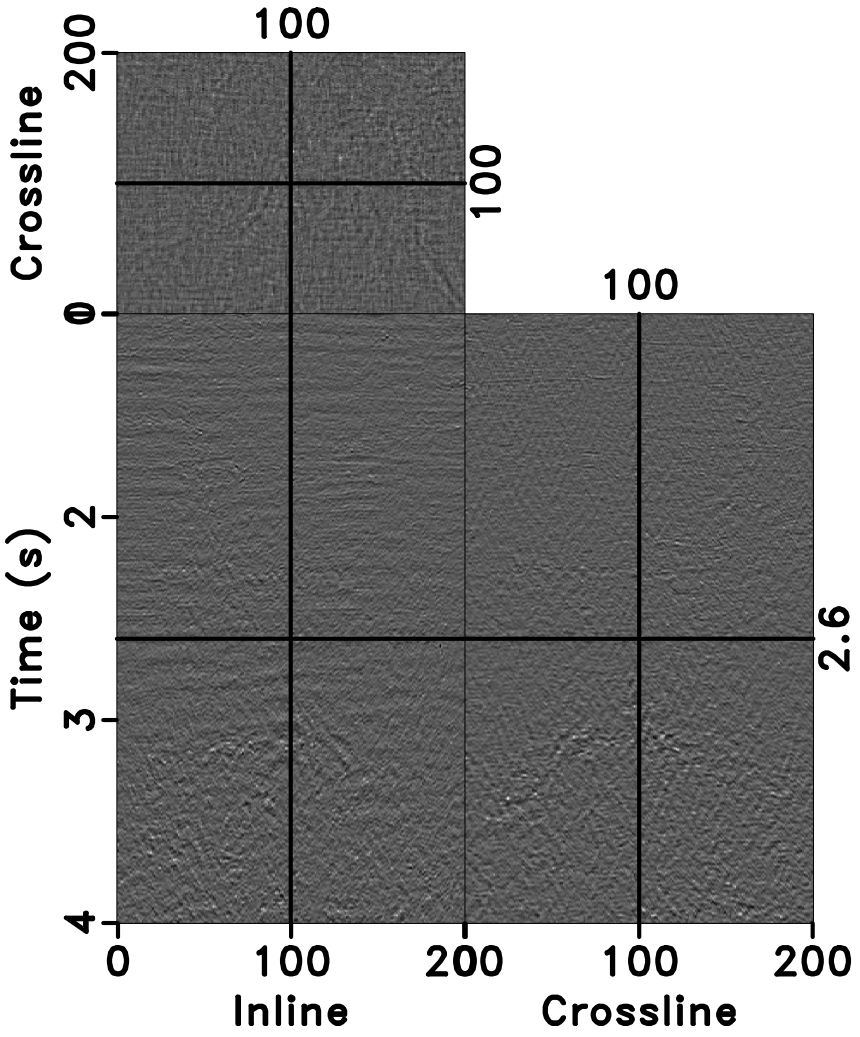

Figure 15: Difference between Figure 10 and Figure 13.

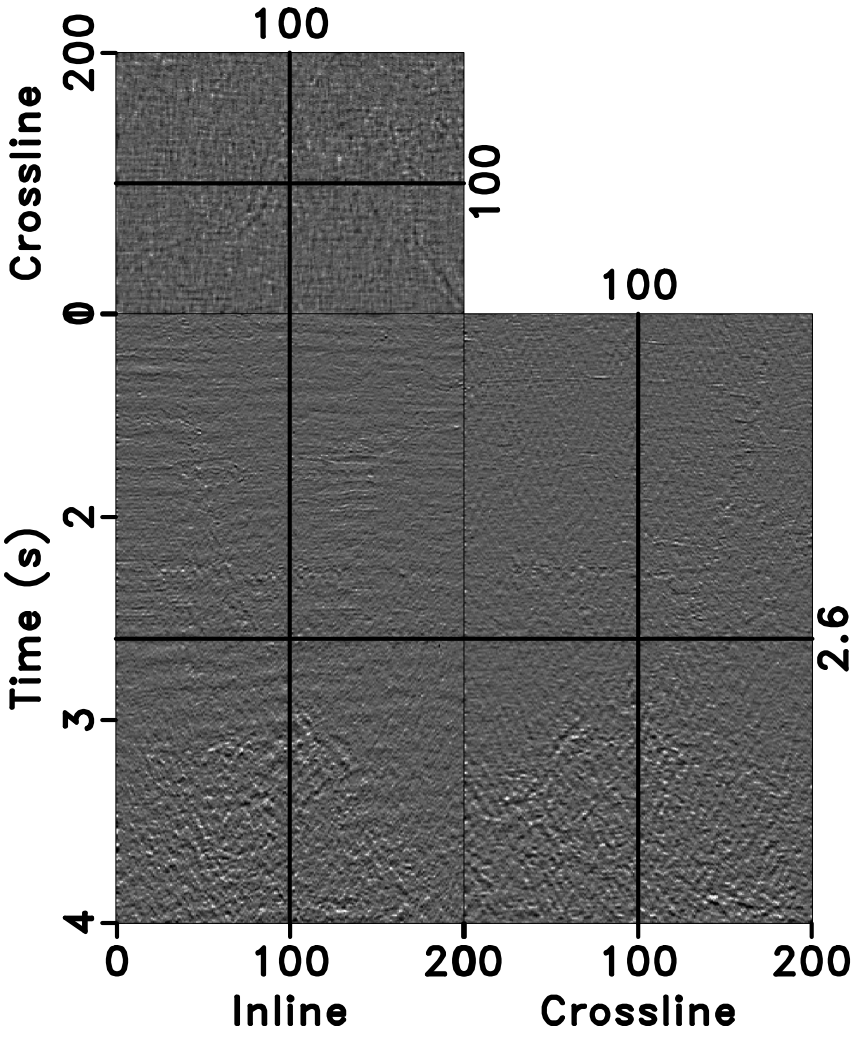

Figure 16: Difference between Figure 10 and Figure 14.

lication is authorized by the Director, Bureau of Economic Geology, The University of Texas at Austin.

APPENDIX A: SIMILARITY-MEAN FILTER

Fomel (2007a) defined local similarity as follows. The global correlation coefficient between two different signals $a(t)$ and $b(t)$ is the functional

$$\gamma = \frac{\langle a(t), b(t) \rangle}{\sqrt{\langle a(t), a(t) \rangle \langle b(t), b(t) \rangle}} \ , \tag{A-1}$$

where $\langle x(t), y(t) \rangle$ denotes the dot product between two signals

$$\langle x(t), y(t) \rangle = \int x(t) y(t) dt \ . \tag{A-2}$$

In a linear algebra notation, the squared correlation coefficient γ from equation A-1 can be represented as a product of two least-squares inverses

$$\gamma^2 = \gamma_1 \gamma_2 \ , \tag{A-3}$$

$$\gamma_1 = (\mathbf{a}^T \mathbf{a})^{-1} (\mathbf{a}^T \mathbf{b}) \ , \tag{A-4}$$

$$\gamma_2 = (\mathbf{b}^T \mathbf{b})^{-1} (\mathbf{b}^T \mathbf{a}) \ , \tag{A-5}$$

where $\mathbf{a}$ is a vector notation for $a(t)$, $\mathbf{b}$ is a vector notation for $b(t)$, and $\mathbf{x}^T \mathbf{y}$ denotes the dot product operation defined in equation A-2. Let $\mathbf{A}$ be a diagonal operator composed of the elements of $\mathbf{a}$ and $\mathbf{B}$ be a diagonal operator composed of the elements of $\mathbf{b}$. Localizing equations A-4 and A-5 amounts to adding regularization to inversion. Scalars γ_1 and γ_2 turn into vectors $\mathbf{c}_1$ and $\mathbf{c}_2$ defined, using shaping regularization (Fomel, 2007b)

$$\mathbf{c}_1 = [\lambda^2 \mathbf{I} + \mathbf{S}(\mathbf{A}^T \mathbf{A} - \lambda^2 \mathbf{I})]^{-1} \mathbf{S} \mathbf{A}^T \mathbf{b} \ , \tag{A-6}$$

$$\mathbf{c}_2 = [\lambda^2 \mathbf{I} + \mathbf{S}(\mathbf{B}^T \mathbf{B} - \lambda^2 \mathbf{I})]^{-1} \mathbf{S} \mathbf{B}^T \mathbf{a} \ , \tag{A-7}$$

where λ scaling controls the relative scaling of operators $\mathbf{A}$ and $\mathbf{B}$. Finally, the componentwise product of vectors $\mathbf{c}_1$ and $\mathbf{c}_2$ defines the local similarity measure.

For using time-dependent smooth weights in the stacking process, the local similarity amplitude can be chosen as a weight for stacking seismic data. We thus stack only those parts of the predicted data whose similarity to the reference one is comparatively large (Liu et al., 2009a).

APPENDEX B: LOWER-UPPER-MIDDLE FILTER

In this appendix, we review lower-upper-middle (LUM) filters introduced by Hardie and Boncelet (1993). Consider a window function containing a set of N samples

centered about the sample $x^\star$. We assume N to be odd. This set of observations will be denoted by $\{x_1, x_2, \cdots, x_N\}$. The rank-ordered set can be written as

$$x_{(1)} \leq x_{(2)} \leq \cdots \leq x_{(N)} \,. \tag{B-1}$$

The estimate of the center sample will be denoted $y^\star$.

Lower-upper-middle smoother

Lower-upper-middle (LUM) smoother is equivalent to center-weighted medians (Justusson, 1981). The output of the LUM smoother with parameter k is given by

$$y^\star = med\{x_{(k)}, x^\star, x_{(N-k+1)}\} \,, \tag{B-2}$$

where $1 \leq k \leq (N+1)/2$.

Thus, the output of the lower-upper-middle (LUM) smoother is $x_{(k)}$ if $x^\star < x_{(k)}$. If $x^\star > x_{(N-k+1)}$, then the output of the LUM smoother is $x_{(N-k+1)}$. Otherwise the output of the LUM smoother is simply $x^\star$.

Lower-upper-middle sharpener

We can define a value centered between the lower- and upper-order statistics, $x_{(l)}$ and $x_{(N-l+1)}$. This midpoint or average, denoted t_l, is given by

$$t_l = (x_{(l)} + x_{(N-l+1)})/2 \,. \tag{B-3}$$

Then, the output of the lower-upper-middle (LUM) sharpener with parameter l is given by

$$y^\star = \begin{cases} x_{(l)}, & \text{if } x_{(l)} < x^\star \leq t_l \\ x_{(N-l+1)}, & \text{if } t_l < x^\star < x_{(N-l+1)} \\ x^\star & \text{otherwise} \end{cases} \,. \tag{B-4}$$

Thus, if $x_{(l)} < x^\star < x_{(N-l+1)}$, then $x^\star$ is shifted outward to $x_{(l)}$ or $x_{(N-l+1)}$ according to which is closest to $x^\star$. Otherwise the sample $x^\star$ is unmodified. By changing the parameter l, various levels of sharpening can be achieved. In the case where $l = (N+1)/2$, no sharpening occurs and the lower-upper-middle (LUM) sharpener is simply an identity filter. In the case where $l = 1$, a maximum amount of sharpening is achieved since $x^\star$ is being shifted to one of the extreme-order statistics $x_{(1)}$ or $x_{(N)}$.

Lower-upper-middle filter

To obtain an enhancing filter that is robust and can reject outliers, the philosophies of the lower-upper-middle (LUM) smoother and lower-upper-middle (LUM) sharpener must be combined. This leads us to the general lower-upper-middle

(LUM) filter. A direct definition is as follows:

$$y^\star = \begin{cases} x_{(k)}, & \text{if } x^\star < x_{(k)} \\ x_{(l)}, & \text{if } x_{(l)} < x^\star < t_l \\ x_{(N-l+1)}, & \text{if } t_l < x^\star < x_{(N-l+1)} \\ x_{(N-k+1)}, & \text{if } x_{(N-l+1)} < x^\star \\ x^\star, & \text{otherwise} \end{cases} . \tag{B-5}$$

where t_l is the midpoint between $x_{(l)}$ and $x_{(N-l+1)}$ defined in equation B-3, and $1 \le k \le l \le (N+1)/2$.

REFERENCES

AlBinHassan, N. M., Y. Luo, and M. N. Al-Faraj, 2006, 3-D edge-preserving smoothing and applications: Geophysics, **71**, P5–P11.

Claerbout, J. F., 1992, Earth Soundings Analysis: Processing Versus Inversion: Blackwell Scientific Publications.

———, 2008, Basic Earth imaging: Stanford Exploration Project, `http://sepwww.stanford.edu/sep/prof/`.

Fehmers, G. C., and C. F. W. Höcker, 2003, Fast structural interpretation with structure-oriented filtering: Geophysics, **68**, 1286–1293.

Fomel, S., 2002, Appliations of plane-wave destruction filters: Geophysics, **67**, 1946–1960.

———, 2007a, Local seismic attributes: Geophysics, **72**, A29–A33.

———, 2007b, Shaping regularization in geophysical estimation problems: Geophysics, **72**, R29–R36.

———, 2008, Predictive painting of 3-D seismic volumes: 78th Annual International Meeting, SEG, Expanded Abstracts, 864–868.

Fomel, S., and A. Guitton, 2006, Regularizing seismic inverse problems by model reparameterization using plane-wave construction: Geophysics, **71**, A43–A47.

Gilboa, G., and S. Osher, 2008, Nonlocal operators with applications to image processing: Multiscale Model & Simulation, **7**, 1005–1028.

Hale, D., 2009, Structure-oriented smoothing and semblance: CWP Report 635, Colorado School of Mines, 261–270.

Hardie, R. C., and C. G. Boncelet, 1993, LUM filters: A class of Rank-Order-Based filters for smoothing and sharpening: IEEE Transactions on Signal Processing, **41**, 1061–1076.

Hoeber, H., S. Brandwood, and D. Whitcombe, 2006, Structurally consistent filtering: Presented at the 68th Annual International Conference and Exhibition, EAGE, Expanded Abstracts.

Justusson, B. I., 1981, Median filtering: Statistical properties: Two-Dimensional Digital Signal Processing, II: Transforms and Median Filters, Springer, 161–196.

Liu, C., Y. Liu, B. Yang, D. Wang, and J. Sun, 2006, A 2D multistage median filter to reduce random seismic noise: Geophysics, **71**, V105–V110.

Liu, G., S. Fomel, L. Jin, and X. Chen, 2009a, Stacking seismic data using local correlation: Geophysics, **74**, V43–V48.

Liu, Y., C. Liu, and D. Wang, 2009b, A 1-D time-varying median filter for seismic random, spike-like noise elimination: Geophysics, **74**, V17–V24.

Mayne, W. H., 1962, Common reflection point horizontal data stacking techniques: Geophysics, **27**, 927–938.

Mi, Y., and G. F. Margrave, 2000, Median filtering in Kirchhoff migration for noisy data: 70th Annual International Meeting, SEG, Expanded Abstracts, 822–825.

Rashed, M. A., 2008, Smart stacking: A new cmp stacking technique for seismic data: The Leading Edge, **27**, 462–467.

Robinson, J. C., 1970, Statistically optimal stacking of seismic data: Geophysics, **35**, 436–446.

Tang, Y., 2007, Selective stacking in the reflection-angle and azimuth domain: 77th Annual International Meeting, SEG, Expanded Abstracts, 2320–2324.

Tomasi, C., and R. Manduchi, 1998, Bilateral filtering for gray and color images: Proceedings of IEEE International Conference on Computer Vision, IEEE, 836–846.

Traonmilin, Y., and P. Herrmann, 2008, Structurally consistent f-x filtering: 78th Annual International Meeting, SEG, Expanded Abstracts, 2642–2646.

Tyapkin, Y., and B. Ursin, 2005, Optimum stacking of seismic records with irregular noise: Journal of Geophysics and Engineering, **2**, 177–187.

Whitcombe, D. N., L. Hodgson, H. Hoeber, and Z. Yu, 2008, Frequency dependent, structurally conformable filtering: 78th Annual International Meeting, SEG, Expanded Abstracts, 2617–2621.

Yilmaz, O., 2001, Seismic data analysis: Processing, inversion, and interpretation of seismic data: SEG.

Zhang, R., and T. J. Ulrych, 2003, Multiple suppression based on the migration operator and a hyperbolic median filter: 73th Annual International Meeting, SEG, Expanded Abstracts, 1949–1952.